

Information on the supplementary animations

The supplementary animations S1-S3 show daily synoptic plots for each of the discussed case studies and further illustrate the interplay of the synoptic systems and the occurrence of the anomalies in the considered surface parameters. S1 shows synoptic plots for DJF 2011/12, S2 shows synoptic plots for DJF 2016/17 and S3 shows synoptic plots for DJF 2012/13. The current date is stated in the figure title (format: YYYYMMDD_HH).

Each plot shows: Daily anomaly of potential temperature at 900 hPa (TH; K, color). Instantaneous sea-level pressure (SLP, grey contour, in intervals of 10 hPa), sea ice edge ($SIC = 0.5$, solid yellow line), climatological sea ice edge ($SIC_{clim} = 0.5$, dashed yellow line), cyclone mask (dashed black contour) and blocking mask (dashed green contour) at 00 UTC on the considered day. The affected sub-region(s) (S1: **KBI** and **KBM**, S2: **KBI**, **KBM** and **KBS**, S3: **ARI** and **KBI**) are marked by orange hatching.

Please note: In the animations, potential temperature is denoted as "TH" and not as " θ " (as it is in the manuscript).

Data detrending

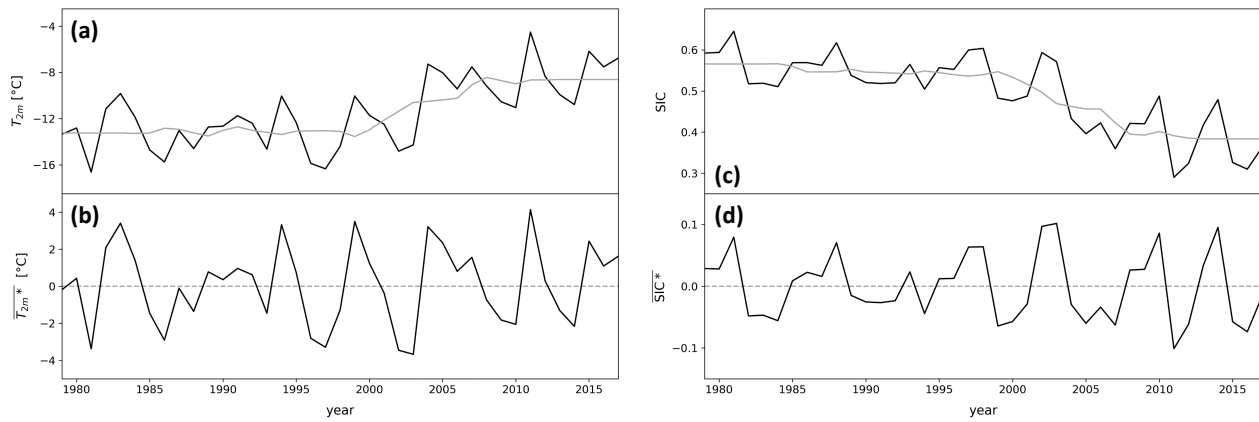


Figure S1. Upper panel: Seasonal mean values (black line) and transient climatology (grey line) of **(a)** T_{2m} (°C) and **(c)** SIC for DJF in the Kara-Barents Seas. Lower panel: Seasonal mean anomalies calculated as difference of seasonal mean values and transient climatology (black line) of **(b)** T_{2m} (T_{2m}^* , °C) and **(d)** SIC (SIC^*).

PCA results (MAM and SON)

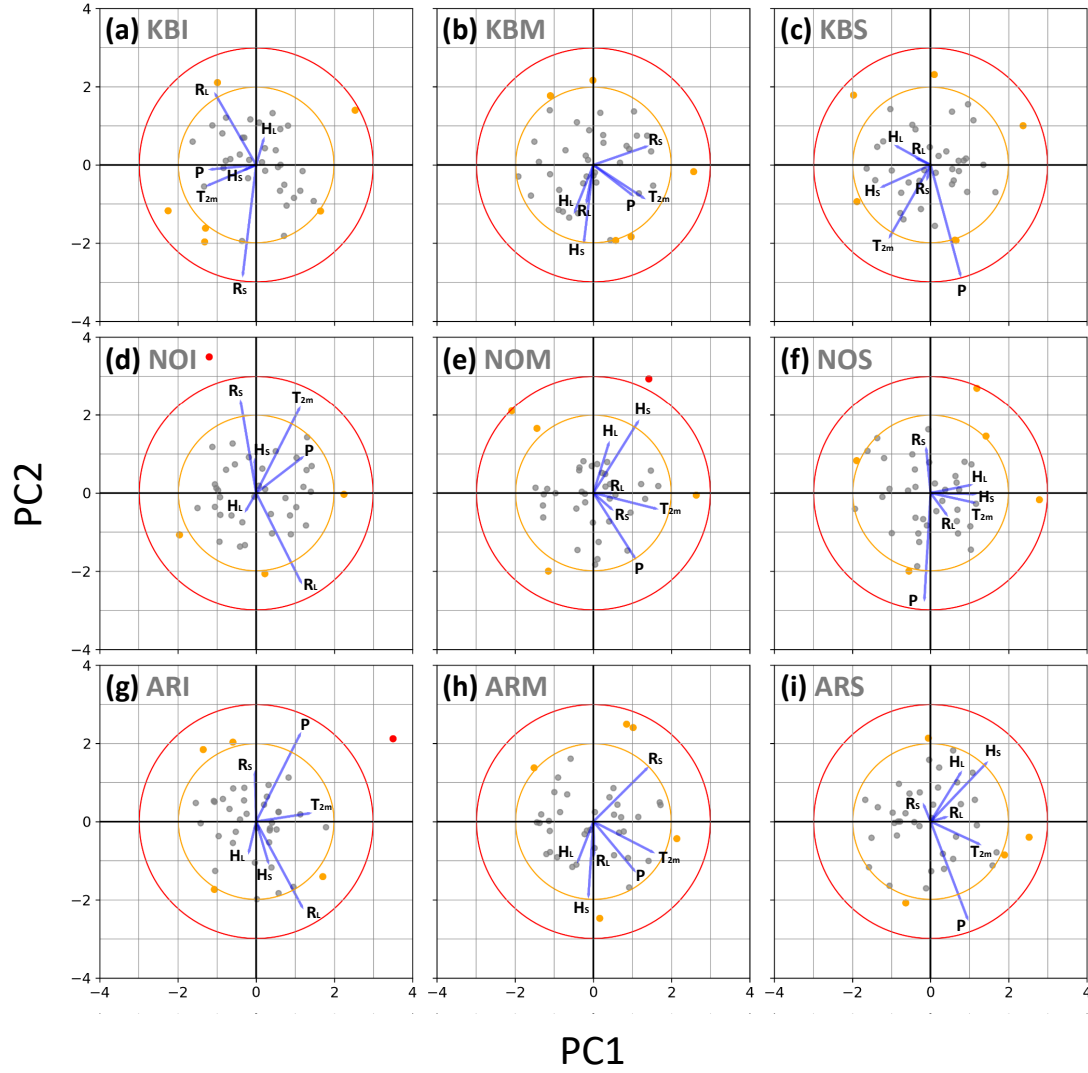


Figure S2. PCA biplot for all sub-regions in MAM with PC1 and PC2 along the x- and y-axis, respectively. Every season is represented by a grey dot, red and orange dots show extreme and anomalous seasons, respectively. Blue lines represent the coefficients of the precursor variables. Red and orange circles represent $d_M=3$ and $d_M=2$, respectively.

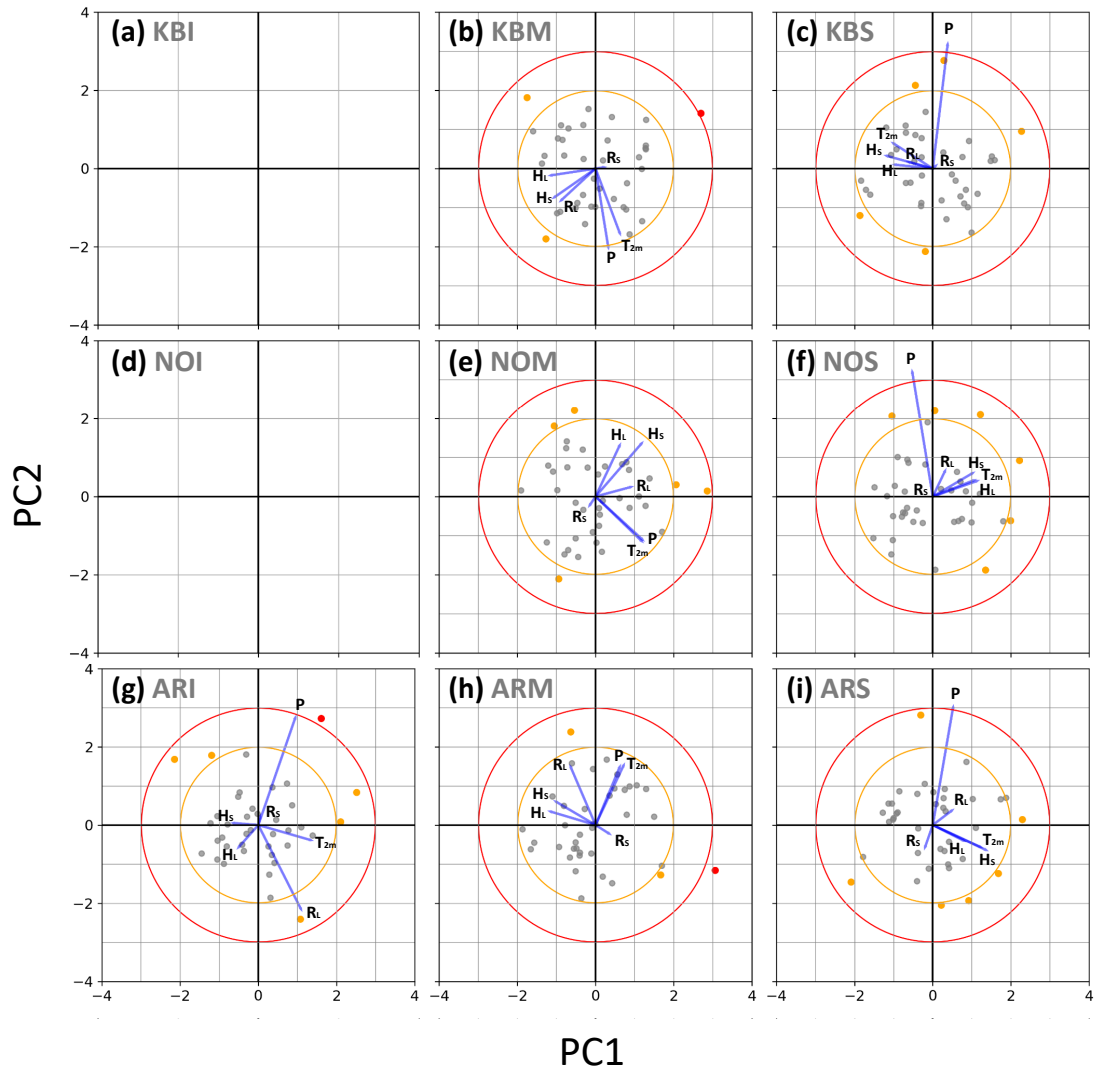


Figure S3. As Fig. S2 but for SON. No biplots are shown for the sub-regions **KBI** and **NOI**, because they fall below the minimum size threshold of 10^5 km^2 in autumn.

Arctic anomalous seasons

20

Season	Sub-regions	d_M	$\overline{T_{2m}^*}$ [K]	$\overline{P^*}$ [mm day ⁻¹]	$\overline{E_S^*}$ [W m ⁻²]	Area [10 ⁵ km ²]
1981/82	ARM	2.1	+1.25 (+0.96)	+0.09 (+0.60)	+10.63 (+1.26)	21.1
	ARS	2.1	+1.14 (+0.64)	-0.69 (-1.45)	+34.06 (+1.45)	
1982/83	KBS	2.6	+2.10 (+1.66)	+0.66 (+2.05)	+16.19 (+0.68)	8.3
	NOI	2.9	+0.05 (+0.03)	+0.46 (+1.01)	-16.61 (-2.95)	
1983/84	ARM	2.1	-2.44 (-1.88)	-0.25 (-1.64)	+11.26 (+1.34)	21.1
	ARS	2.3	-4.42 (-2.48)	-0.54 (-1.14)	-31.91 (-1.36)	
1984/85	NOM	2.3	+4.34 (+2.73)	+0.42 (+1.02)	+11.23 (+0.43)	34.0
	NOS	2.1	+1.17 (+2.45)	-0.60 (-1.32)	+29.50 (+1.64)	
1985/86	NOI	2.3	-2.19 (-1.06)	-0.78 (-1.69)	+8.01 (+1.42)	50.4
	NOS	2.1	-0.37 (-0.77)	-0.68 (-1.50)	-4.69 (-0.26)	
	ARM	2.5	+3.28 (+2.52)	+0.32 (+2.06)	-10.32 (-1.23)	
	ARS	2.8	+3.69 (+2.07)	+0.71 (+1.49)	+63.00 (+2.68)	
1986/87	KBS	2.0	-1.97 (-1.56)	-0.09 (-0.29)	-54.00 (-2.28)	6.7
1988/89	NOI	2.3	-4.39 (-2.12)	-0.40 (-0.88)	-8.72 (-1.55)	1.5
1992/93	KBS	2.0	+0.83 (+0.66)	+0.63 (+1.96)	+4.85 (+0.21)	12.9
	NOM	2.1	-0.75 (-0.47)	+0.28 (+0.67)	-58.47 (-2.22)	
1993/94	ARI	2.4	-0.60 (-1.02)	-0.09 (-1.85)	+1.50 (+0.42)	82.3
1995/96	NOS	2.3	+0.12 (+0.24)	-0.93 (-2.05)	+28.35 (+1.58)	27.8
1996/97	KBS	2.3	-1.88 (-1.50)	+0.50 (+1.54)	-56.87 (-2.40)	13.0
	NOM	2.3	-2.23 (-1.40)	-0.64 (-1.55)	+39.35 (+1.49)	
2000/01	NOS	2.2	+0.11 (+0.23)	-0.99 (-2.18)	+7.99 (+0.45)	27.8
2005/06	NOS	2.1	+0.81 (+1.69)	-0.12 (-0.27)	+36.78 (+2.05)	27.8
2011/12	KBI	2.5	+6.65 (+2.64)	+0.26 (+2.01)	+5.94 (+0.62)	16.0
	KBM	2.7	+4.72 (+1.74)	-0.01 (-0.06)	+28.41 (+1.59)	
2012/13*	ARI	2.8	-1.27 (-2.15)	-0.11 (-2.41)	-5.58 (-1.55)	82.3
2013/14	KBI	2.8	-3.80 (-1.51)	-0.32 (-2.45)	+17.02 (+1.77)	5.4
2014/15	NOS	2.3	-0.67 (-1.40)	+0.86 (+1.89)	-42.95 (-2.39)	27.8
2015/16	ARI	2.1	-0.18 (-0.31)	-0.02 (-0.43)	+6.59 (+1.83)	82.3
2017/18	NOI	2.1	+2.12 (+1.02)	+0.64 (+1.40)	+10.47 (+1.86)	83.8
	ARI	2.0	+1.34 (+2.27)	+0.01 (+0.29)	+6.24 (+1.74)	

Table S1. Anomalous seasons for DJF, including the affected sub-regions and respective Mahalanobis distance d_M , the seasonal mean anomalies of T_{2m} , P and E_S (standardized seasonal mean anomalies in brackets) and total affected area. Seasons labeled with an asterisk occur as extreme seasons in one or several other sub-region(s) (see Table 2 in the main paper).

Season	Sub-regions	d_M	$\overline{T_{2m}^*}$ [K]	$\overline{P^*}$ [mm day ⁻¹]	$\overline{E_S^*}$ [W m ⁻²]	Area [10 ⁵ km ²]
1980	KBS	2.2	-0.36 (-0.61)	-0.60 (-2.26)	-3.39 (-0.63)	25.5
	ARI	2.1	-0.24 (-1.33)	+0.13 (+0.69)	-1.49 (-0.44)	
1981	KBS	2.2	-0.24 (-0.41)	+0.40 (+1.50)	+2.03 (+0.37)	11.2
1983	NOS	2.2	-0.43 (-1.15)	+0.59 (+2.67)	-6.96 (-1.87)	30.4
1985	KBS	2.1	+0.02 (+0.03)	-0.50 (-1.91)	+6.97 (+1.29)	11.2
1987	NOM	2.2	-0.16 (-0.50)	-0.75 (-2.27)	+4.00 (+0.71)	35.5
	NOS	2.2	-0.10 (-0.27)	-0.49 (-2.24)	-3.95 (-1.06)	
1989	ARI	2.5	+0.26 (+1.42)	+0.44 (+2.40)	-0.63 (-0.19)	14.3
1991	ARS	2.1	+0.54 (+1.42)	-0.37 (-1.45)	+6.92 (+2.01)	13.5
1992	ARS	2.4	-0.56 (-1.47)	-0.40 (-1.57)	-1.92 (-0.56)	13.5
1993	KBM	2.0	-0.11 (-0.26)	-0.40 (-2.05)	+4.59 (+0.80)	11.6
1994	ARI	2.2	+0.08 (+0.45)	+0.37 (+2.00)	+1.25 (+0.37)	14.3
1995	KBM	2.4	+0.91 (+2.20)	+0.22 (+1.10)	+16.82 (+2.92)	22.8
	KBS	2.1	+0.31 (+0.52)	+0.58 (+2.22)	-1.97 (-0.36)	
1996	ARI	2.1	-0.13 (-0.71)	+0.15 (+0.82)	-4.75 (-1.40)	89.9
	ARM	2.0	-0.18 (-1.10)	+0.05 (+0.64)	-7.35 (-2.03)	
1998	ARM	2.4	+0.45 (+2.71)	+0.01 (+0.13)	+8.85 (+2.44)	75.6
1999	KBM	2.3	-0.51 (-1.23)	+0.24 (+1.22)	-9.08 (-1.58)	25.1
	ARS	2.4	-0.68 (-1.81)	+0.46 (+1.81)	-0.74 (-0.22)	
2000	NOM	2.7	-0.65 (-2.01)	-0.56 (-1.69)	-5.63 (-1.00)	35.5
	NOS	2.2	-0.67 (-1.78)	-0.37 (-1.69)	-1.12 (-0.30)	
2002	ARS	2.5	-0.13 (-0.34)	-0.47 (-0.86)	+5.04 (+1.47)	13.5
2003	NOS	2.4	+0.98 (+2.61)	-0.16 (-0.72)	+3.60 (+0.96)	30.4
2004	ARM	2.7	-0.01 (-0.04)	-0.06 (-0.76)	-2.57 (-0.71)	86.8
	KBS	2.1	+0.52 (+0.89)	-0.23 (-0.89)	+12.26 (+2.26)	
2005	ARM	2.1	+0.13 (+0.77)	-0.06 (-0.71)	+0.90 (+2.47)	75.6
2006	KBM	2.1	+0.43 (+1.04)	+0.40 (+2.03)	+3.04 (+0.53)	11.6
2007	ARM	2.2	+0.34 (+2.05)	-0.06 (-0.73)	+9.47 (+2.61)	75.6
2008	ARS	2.4	-0.37 (-0.97)	-0.41 (-1.60)	+1.35 (+0.39)	13.5
2011	ARS	2.2	-0.41 (-1.08)	+0.63 (+2.49)	-0.57 (-1.04)	13.5
2013*	KBS	2.8	+1.64 (+2.79)	-0.05 (-0.18)	+15.45 (+2.85)	11.2
2016*	KBS	2.4	+1.69 (+2.88)	+0.16 (+0.61)	-1.03 (-0.19)	100.3
	ARM	2.1	+0.13 (+0.78)	+0.14 (+1.74)	+3.36 (+0.93)	
	ARS	2.2	+0.88 (+2.34)	-0.34 (-1.32)	+2.57 (+0.75)	
2018	NOS	2.1	+0.04 (+0.10)	+0.51 (+2.35)	-0.44 (-0.12)	30.4

Table S2. Same as Table S1, but for JJA.

Season	Sub-regions	d_M	$\overline{T_{2m}^*}$ [K]	$\overline{P^*}$ [mm day ⁻¹]	$\overline{E_S^*}$ [W m ⁻²]	Area [10 ⁵ km ²]
1981	KBS	2.6	-2.58 (-2.86)	+0.25 (+1.04)	-43.72 (-2.14)	5.9
1987	KBS	2.3	-1.23 (-1.36)	-0.40 (-1.67)	-3.12 (-0.15)	5.9
1986	ARM	2.6	+0.41 (+0.56)	-0.08 (-0.58)	-7.07 (-1.24)	19.9
1988	NOM	2.2	-2.26 (-2.05)	-0.65 (-1.52)	+1.83 (+0.15)	5.8
1989	KBM	2.1	+1.76 (+1.16)	+0.25 (+1.93)	+19.83 (+1.62)	16.8
	KBS	2.1	+1.56 (+1.73)	-0.04 (-0.15)	+43.98 (+2.16)	
1990*	KBI	2.4	+2.38 (+1.61)	+0.21 (+1.70)	+4.73 (+1.38)	31.8
	KBS	2.0	+0.53 (+0.59)	+0.36 (+1.51)	-11.80 (-0.58)	
	ARM	2.5	+0.71 (+0.96)	+0.14 (+1.05)	+8.78 (+1.54)	
1992	ARI	2.1	-0.11 (-0.13)	+0.02 (+0.23)	-3.15 (-1.65)	100.8
	ARM	2.1	-1.18 (-1.60)	-0.20 (-1.50)	-10.55 (-1.85)	
1993	ARI	2.0	-0.84 (-0.95)	-0.12 (-1.90)	+0.52 (+0.27)	80.9
1994	NOI	2.1	-1.04 (-0.75)	-0.04 (-0.10)	-0.96 (-0.30)	1.3
1995	KBI	2.5	+3.10 (+2.10)	+0.23 (+1.88)	+6.60 (+1.93)	97.8
	KBM	2.6	+2.77 (+1.83)	+0.29 (+2.18)	+9.06 (+0.74)	
	ARI	2.2	+0.87 (+0.98)	+0.06 (+0.84)	+2.84 (+1.48)	
1996*	NOS	2.9	+0.23 (+0.55)	-0.63 (-2.90)	+21.12 (+1.67)	50.8
	ARM	2.2	+1.60 (+2.16)	+0.23 (+1.71)	+3.22 (+0.56)	
	ARS	2.5	+2.21 (+2.17)	+0.53 (+1.60)	+32.84 (+1.81)	
1997	NOS	2.1	-0.37 (-0.89)	+0.39 (+1.81)	-8.05 (-0.64)	28.3
2000	KBS	2.0	+0.54 (+0.60)	+0.39 (+1.65)	-15.98 (-0.78)	11.7
	NOM	2.3	-0.78 (-0.71)	+0.37 (+0.87)	-28.27 (-2.24)	
2001	NOI	2.2	-3.59 (-2.61)	-0.61 (-1.42)	+0.38 (+0.12)	9.7
	NOM	2.9	-3.18 (-2.88)	-0.89 (-2.08)	-0.40 (-0.03)	
	ARS	2.1	+0.20 (+0.19)	-0.71 (-2.14)	+15.84 (+0.87)	
2004	KBS	2.7	+0.73 (+0.81)	-0.63 (-2.64)	+40.66 (+1.99)	43.9
	NOI	2.2	+2.72 (+1.97)	+0.77 (+1.80)	+4.03 (+1.25)	
	NOM	2.6	+2.51 (+2.28)	+0.84 (+1.96)	+27.70 (+2.20)	
	NOS	2.8	+1.16 (+2.78)	-0.07 (-0.31)	+34.71 (+2.74)	
	ARS	2.2	+0.03 (+0.03)	+0.33 (+1.00)	-32.31 (-1.78)	
2008	KBM	2.2	-0.90 (-0.59)	-0.15 (-1.16)	-25.10 (-2.05)	10.9
2009	ARI	2.3	-0.98 (-1.10)	-0.02 (-0.26)	-5.59 (-2.92)	80.9
2010	ARS	2.1	+1.69 (+1.67)	+0.57 (+1.72)	+19.81 (+1.10)	2.6
2011	KBI	2.1	+2.34 (+1.58)	+0.12 (+0.94)	+6.96 (+2.03)	25.9
	ARM	2.6	+0.02 (+0.03)	-0.06 (-0.41)	-7.21 (-1.26)	
2013	KBI	2.0	-2.03 (-1.38)	-0.19 (-1.56)	-6.07 (-1.78)	34.3
	NOS	2.1	-0.81 (-1.93)	-0.11 (-0.50)	-22.09 (-1.74)	
2015	KBI	2.3	+1.08 (+0.73)	+0.06 (+0.53)	+5.02 (+1.47)	16.9
	KBM	2.0	+1.91 (+1.26)	+0.13 (+1.02)	+20.87 (+1.70)	
2016	NOS	2.0	+0.43 (+1.02)	-0.36 (-1.67)	+22.17 (+1.75)	28.3
2018	KBI	2.9	-4.04 (-2.74)	-0.27 (-2.19)	-8.18 (-2.39)	16.9
	KBM	2.1	-2.79 (-1.84)	-0.08 (-0.61)	-28.04 (-2.29)	

Table S3. Same as Table S1, but for MAM.

Season	Sub- regions	d_M	$\overline{T_{2m}^*}$ [K]	$\overline{P^*}$ [mm day ⁻¹]	$\overline{E_S^*}$ [W m ⁻²]	Area [10 ⁵ km ²]
1981	ARI	2.6	+1.35 (+1.13)	-0.06 (-0.60)	+3.32 (+1.92)	32.3
1984	KBS	2.1	+0.55 (+0.67)	-0.72 (-2.21)	-6.59 (-0.36)	75.8
	NOS	2.1	+0.70 (+1.61)	-0.43 (-1.38)	+22.96 (+1.76)	
	ARI	2.1	+2.72 (+2.28)	+0.14 (+1.40)	-1.23 (-0.72)	
1987	ARI	2.7	-2.44 (-2.04)	-0.06 (-0.55)	-3.87 (-2.24)	32.3
1988	KBS	2.5	-1.93 (-2.33)	+0.58 (+1.77)	-31.94 (-1.75)	16.4
	NOM	2.3	-2.09 (-1.49)	-0.73 (-1.53)	+11.70 (+1.08)	
	ARS	2.1	+0.19 (+0.32)	-0.39 (-1.90)	+5.93 (+0.82)	
1990	ARM	2.1	+0.20 (+0.21)	-0.01 (-0.08)	-9.51 (-2.17)	52.7
1991	ARS	2.1	+0.84 (+1.39)	-0.26 (-1.29)	+4.97 (+0.69)	18.5
1992	NOM	2.1	+1.81 (+1.29)	+0.68 (+1.43)	+17.83 (+1.64)	4.2
1993	ARS	2.8	-0.60 (-0.99)	+0.54 (+2.64)	-5.98 (-0.83)	18.5
1994	NOM	2.1	-2.78 (-1.99)	-0.65 (-1.38)	+4.90 (+0.45)	36.4
	ARI	2.2	-1.34 (-1.12)	+0.05 (+0.53)	-1.17 (-0.68)	
1996	NOM	2.3	+0.93 (+0.66)	+0.30 (+0.63)	-23.07 (-2.12)	4.2
1998	KBM	2.5	-3.44 (-2.12)	-0.40 (-1.96)	+11.80 (+1.30)	10.7
1999	KBM	2.2	-0.07 (-0.04)	+0.35 (+1.70)	+14.86 (+1.64)	42.0
	NOS	2.2	+0.31 (+0.72)	+0.63 (+2.03)	+4.71 (+0.36)	
2000	KBS	2.2	+1.48 (+1.80)	-0.58 (-1.77)	+28.90 (+1.59)	12.2
2002	NOS	2.3	+0.40 (+0.93)	-0.69 (-2.24)	+12.12 (+0.93)	31.3
2005	KBS	2.2	+0.85 (+1.03)	+0.62 (+1.89)	+10.33 (+0.57)	12.2
2006	ARS	2.1	+0.61 (+1.02)	-0.10 (-0.50)	+15.04 (+2.09)	18.5
2007*	NOS	2.3	-0.47 (-1.08)	+0.73 (+2.36)	-4.74 (-0.36)	31.3
2009	ARS	2.6	-0.83 (-1.36)	-0.42 (-2.04)	-13.21 (-1.83)	18.5
2010	ARS	2.3	+1.48 (+2.44)	+0.18 (+0.90)	+12.73 (+1.77)	18.5
2011	NOS	2.4	+0.65 (+1.49)	+0.43 (+1.39)	+20.50 (+1.57)	31.3
2016	NOM	2.9	+3.43 (+2.45)	+0.82 (+1.73)	+24.57 (+2.26)	120.5
	NOS	2.4	+0.98 (+2.27)	-0.02 (-0.08)	+28.64 (+2.20)	
	ARI	2.7	+2.94 (+2.46)	+0.24 (+2.34)	+0.12 (+0.07)	
	ARM	2.5	+1.90 (+2.01)	+0.06 (+0.75)	+7.65 (+1.75)	
2018*	KBS	2.8	+0.45 (+0.55)	+0.89 (+2.73)	-1.76 (-0.10)	12.2

Table S4. Same as Table S1, but for SON.

Sea ice transport during DJF 2016/17

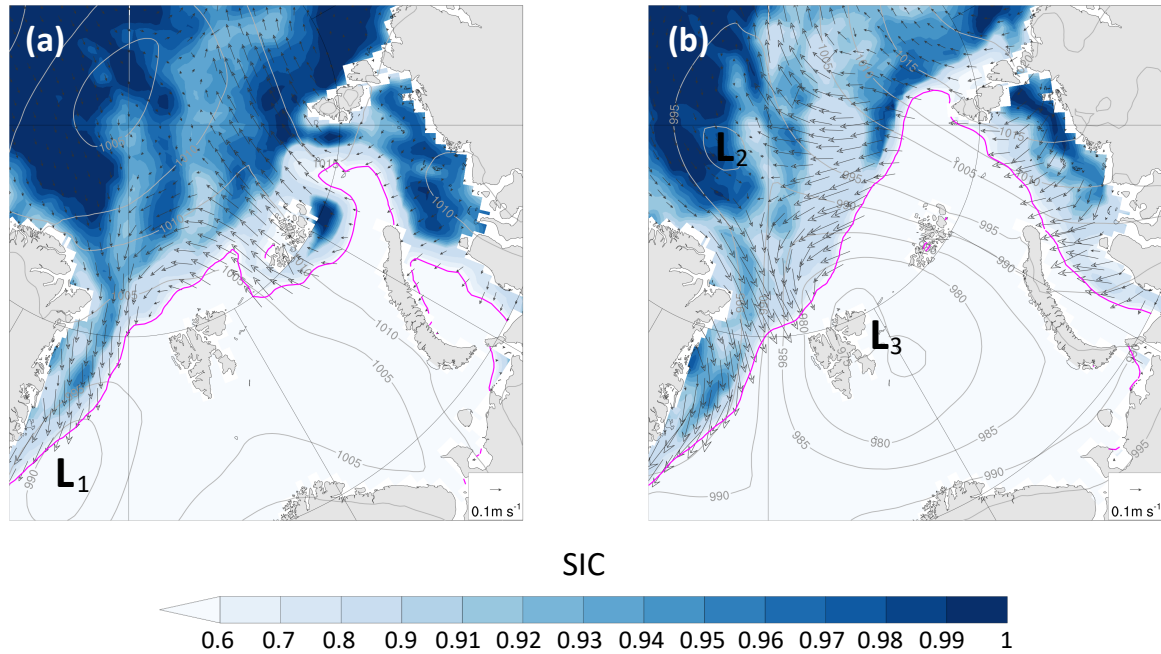


Figure S4. Daily mean SIC (color, note the irregular contour intervals) and sea ice transport vectors from PIOMAS (in m s^{-1}) as well as instantaneous sea ice edge (SIC = 0.5, pink line) and SLP (grey contour, in intervals of 5 hPa) at 00 UTC on (a) 17 December 2016 and (b) 24 December 2016 in the region of the Kara-Barents Seas. Labels mark the positions of surface cyclones (L_1 - L_3).

Figure S4 shows the influence of several surface cyclones on the sea ice transport in the Kara-Barents Seas during the extreme winter 2016/17, leading to a strong reduction of SIC between 18 December and 23 December 2016 (see Fig. 10c in the main paper). Figure S4a shows the situation before this event on 17 December, when a first cyclone (L_1) approaches the region from the Nordic Seas and the sea ice edge still extends to the South of Franz Josef Land. During the following days, the wind field and warm air advection associated with the cyclones L_1 and L_2 , travelling from the Nordic Seas into the High Arctic, and L_3 , which becomes stationary in the Barents Seas (see supplementary animation S2 and blue heatmap in Fig. 10 in the main paper), result in a strong retreat of the sea ice edge in the northern part of the Barents Sea. The remains of cyclone L_2 as well as cyclone L_3 on 24 December are shown in Fig. S4b along with the reduction in SIC, which leads to a higher mobility of the sea ice in the High Arctic and thus stronger sea ice transport in this region.